Unimpeded tunneling in graphene nanoribbons



2010 J. Phys.: Condens. Matter 22 165301

(http://iopscience.iop.org/0953-8984/22/16/165301)

J. Phys.: Condens. Matter **22** (2010) 165301 (6pp) doi:10.1088/0953-8984/22/16/165301

# Unimpeded tunneling in graphene nanoribbons

**O Roslyak[1], A Iurov[1], Godfrey Gumbs[1,2] and Danhong Huang[3]**

[1] Department of Physics and Astronomy, Hunter College of City University of New York, 695 Park Avenue, New York, NY 10065-50085, USA
[2] Donostia International Physics Center (DIPC), Paseo de Manuel Lardizabal, 4, 20018 San Sebastián, Basque Country, Spain
[3] Air Force Research Laboratory (AFRL/RVSS), Kirtland Air Force Base, NM 87117, USA

Received 11 February 2010, in final form 4 March 2010
Published 30 March 2010
Online at stacks.iop.org/JPhysCM/22/165301

**Abstract**
We studied the Klein paradox in zigzag (ZNR) and anti-zigzag (AZNR) graphene nanoribbons. Due to the fact that ZNR (the number of lattice sites across the nanoribbon = $N$ is even) and AZNR ($N$ is odd) configurations are indistinguishable when treated by the Dirac equation, we supplemented the model with a pseudo-parity operator whose eigenvalues correctly depend on the sublattice wavefunctions for the number of carbon atoms across the ribbon, in agreement with the tight-binding model. We have shown that the Klein tunneling in zigzag nanoribbons is related to conservation of the pseudo-parity rather than pseudo-spin as in infinite graphene. The perfect transmission in the case of head-on incidence is replaced by perfect transmission at the center of the ribbon and the chirality is interpreted as the projection of the pseudo-parity on momentum at different corners of the Brillouin zone.

(Some figures in this article are in colour only in the electronic version)

Nanoelectronics based on graphene has become a fast growing field [1, 2] with a number of technical applications [3]. Electron/hole low energy dynamics is described by the Dirac equation valid around the corners of the Brillouin zone (Dirac $K$ ($K'$) points) [4–6]. One of the most striking consequences of the massless nature of the carriers is the so-called Klein paradox, which is the unimpeded penetration through high and wide potential barriers [1, 7], as shown in figure 1. Graphene provides a convenient medium for experimental verification of the effect. The underlying physics of Klein tunneling is based on the notion of chirality as a symmetry between electrons and holes in graphene. Formally, each of the branches of the dispersion conical section is characterized by a specific sign of the pseudo-spin projection on to the momentum. The Klein effect is related to the conservation of this quantity across the potential barrier.

In this paper, we explore the notion that chirality is necessary for Klein tunneling. For this one must compare transport in systems which provide either chiral or non-chiral massless Dirac fermions, such as graphene nanoribbons (GNR). These are just infinitely long carbon nanotubes unzipped along either an armchair (ANR) or zigzag (ZNR) direction and then flattened. The ANR boundary conditions mix the valleys at $K$ ($K'$) points giving a dispersion strongly dependent on the number of carbon atoms ($N$) across the ribbon (modulo 3) [8] and producing semi-metallic or insulating subbands. The fermions in the ANR are chiral and the potential barrier is perfectly transparent to electron scattering at angles close to normal incidence, in agreement with the Klein effect in the graphene sheets. This makes ANR a basis for graphene switches, random access memory and GNR field-effect transistors. When the electron motion is confined by a zigzag edge, surface states describe the lowest energy bands of the ZNR providing the right (left) transmission channels [9, 10] at $K$ ($K'$), as shown in figure 1. Transmission through the barrier is possible if the gate potential acts as an inter-valley scattering source. Unlike the ANR, the ZNR lowest energy dispersion does not show substantial dependence on $N$. However, the transmission drastically depends on this parameter. In the single channel regime, it has been predicted that the transmission is allowed (forbidden) for odd (even) $N$. This suggests referring to the case with an odd number of atoms as an anti-zigzag nanoribbon (AZNR) [11]. This current blocking was originally interpreted in analogy with the spin-valve effect in ferromagnetic junctions, thereby gaining the name of valley-valve effect [12, 13]. Later, however, it was attributed to symmetric (asymmetric) coupling of states localized at opposite edges (sublattices) of the

 

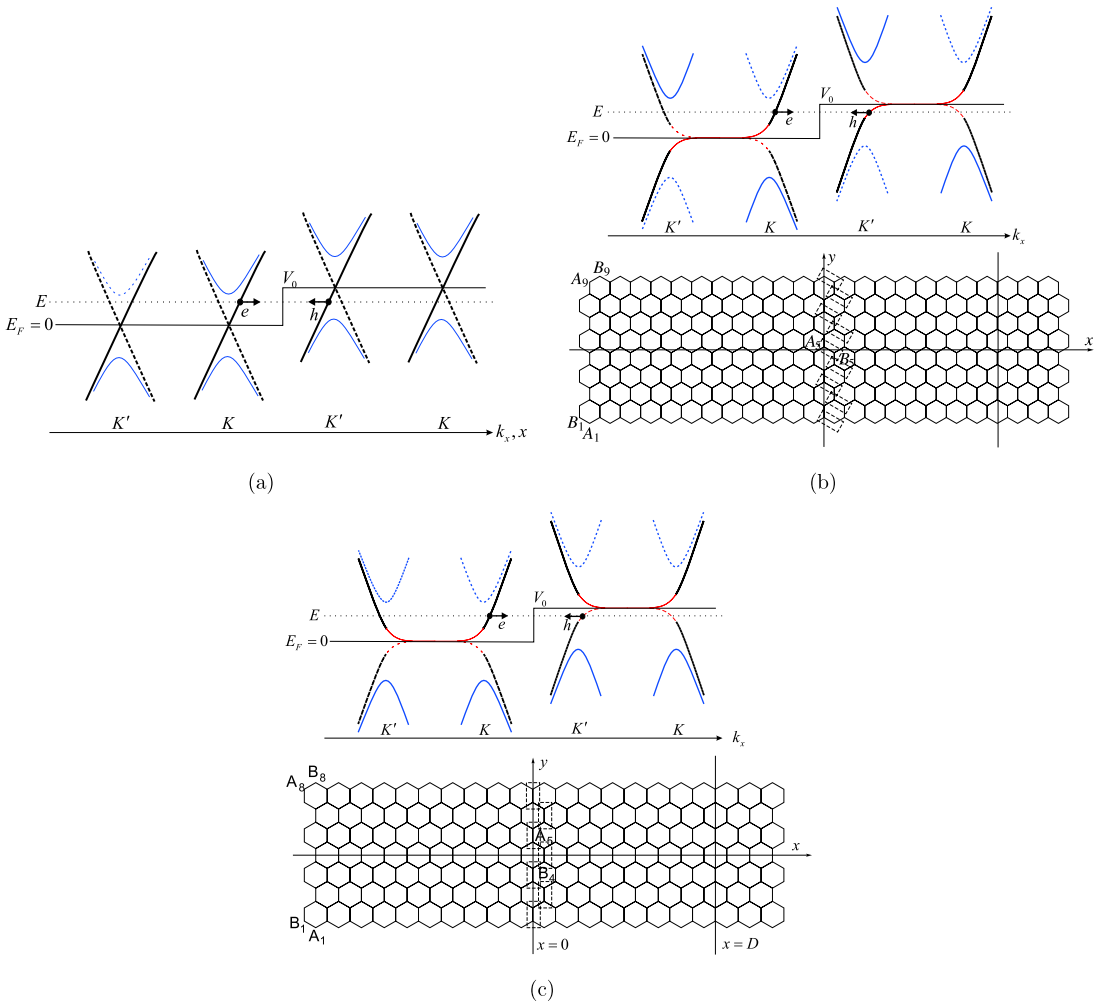


**Figure 1.** Panel (a) shows an infinite graphene n–p–n junction and its corresponding chiral dispersion curves. The $\pi, \pi^\star$ bands are depicted by black lines; the nearby parabolic shaped (blue) curves denote $\mathcal{V}, \mathcal{V}^\star$ bands. The different values of the pseudo-spin projected on the momentum (eigenvalues of $\sim\sigma \cdot p$ given by $s_B p_x/|p|$) are shown in solid and dashed curves. Panel (b) describes the 9-AZNR n–p–n junction and its chiral particle dispersion. The two different values of pseudo-parity projection on the pseudo-spin $1 - s^\star \cdot \eta$ are presented in solid (dashed) curves. Panel (c) shows the 8-ZNR configuration and its non-chiral dispersion curves. For all panels dashed rectangles represent the unit cells.

GNR [14]. Owing to the fact that the model for the ZNR and AZNR configurations are indistinguishable at the level of the Dirac equation [15], the latter must be augmented with a pseudo-parity operator whose eigenvalues provide the correct dependence (in agreement with the tight-binding model) of the sublattice wavefunctions on $N$. Bellow, we show that when it comes to Klein tunneling in AZNR, pseudo-parity plays the role of the pseudo-spin in infinite graphene. Perfect transmission in the case of head-on incidence is replaced by perfect transmission at the center of the ribbon. The chirality in AZNR is related to the projection of the pseudo-parity on the pseudo-spin around $K_x$ and $K'_x$.

The energy band structure of GNR depends on the shape of their edges. We shall focus on the ZNR configuration since the fermions in this geometry are not chiral [15]. At $K$, $(K')$ points, there is an excess right (left) moving conducting channel for $\pi(\pi^\star)$ bands. In the spirit of the single channel regime [10], these bands alone will be considered further. Conventionally, these are given by the $\mathbf{k}\cdot\mathbf{p}$ approximation for the tight-binding model [1], yielding the following electron + (hole −) dispersion valleys: $V(x) - E = \pm\sqrt{k_x^2 - k_y^2}$. Here the energy is measured in units of the hopping parameter $t = 2.7\sqrt{3}/2$ eV between nearest-neighbor carbon atoms, and the wavevectors are in units of the inverse distance between them $a_0 = 1.42$ Å. The hard-wall boundary conditions mix the transverse and the longitudinal electron momenta $k_x = k_y \coth(Wk_y)$, where the GNR width is $W = 2N - 1$ for an even number $N$ of carbon atoms across the ribbon and $W = \frac{3}{2}(N - 1)$, otherwise. The chemical potential provided by the underlying metal contact (insulating strip, carbon nanotube) [16, 17] assumes the form of a sharp n–p–n junction: $V(x) = V_0[\theta_+(x) - \theta_+(x - D)]$. In this notation, $V_0$ is the height of the potential barrier and $\theta_+(x)$ is the Heaviside step function.

As shown in figure 1, this alternating doping provides scattering (p-doped) region sandwiched in between left (right) leads (n-doped). The electric current through the potential

barrier is given by the incident electron of energy $E$ in the range $[0, \Delta]$, where $2\Delta$ is the energy separation between the top of the next highest valence band and the bottom of the next lowest conduction band (the parabolically shaped $\mathcal{V}$, ($\mathcal{V}^\star$) bands in figure 1). To stay in the single channel regime, where the scattering occurs within the lowest conduction $\pi$ and highest valence $\pi^\star$ bands, we require the barrier height $V_0$ in the range $|E - V_0| \leqslant \Delta$.

The scattering problem with the sharp edge junction is fully determined by the wavefunction for the $\pi$ and $\pi^\star$ bands. The corresponding eigenfunctions for the two sublattices $(A, B)$ can be factorized into the element-wise product of longitudinal, transverse, pseudo-parity and electron–hole parity two component wavefunctions as

$$\Psi_{\pm K,N}(x, y) = \begin{pmatrix} \Psi_A \\ \Psi_B \end{pmatrix} = \phi_{\pm K}(x) \circ \chi(y) \circ \eta_{\pm K} \circ s. \quad (1)$$

Here, the longitudinal wavefunction depends on the parity $X_N$ of the number of carbon atoms across the ribbon:

$$\phi_{\pm K,N}(x) = \frac{1}{\sqrt{2\pi}} \begin{pmatrix} \exp(\pm \mathrm{i}(K + k_x)x) \\ \exp(\pm \mathrm{i}(K + k_x)(x + X_N)) \end{pmatrix}, \quad (2)$$

where $X_N = 0$ for $N$ being even and $X_N = \sqrt{3}/2$ for $N$ being odd. Its presence stems from the suitable shape of the unit cells as depicted in figure 1. The choice of $\pm$ defines the right (transmitted) and the left (reflected) movers (direction of the electron group velocity for $E–V(x) > 0$), respectively. The shape of the unit cells and, consequently, the form of the longitudinal wavefunction ascertains the translational symmetry of the wavefunction (1) along the ribbon. The transverse wavefunction component is

$$\chi(y) = \left(\frac{2k_y}{\sinh(2Wk_y) - 2Wk_y}\right)^{1/2} \begin{pmatrix} \sinh[k_y(W/2 + y)] \\ \sinh[k_y(W/2 - y)] \end{pmatrix}, \quad (3)$$

which satisfies the Dirac equation at $\pm K = \pm 2\pi/3\sqrt{3}$ as well as the hard-wall boundary conditions across the ribbon. In contrast to infinite graphene or the ANR, these bands describe localized bound edge states for $\Im m\ Wk_y = 0$ and delocalized bulk states for $\Re e\ Wk_y = 0$, $\Im m\ Wk_y \leqslant \pi$; while $\mathcal{V}(\mathcal{V}^\star)$ bands correspond to $\Re e\ Wk_y = 0$, $\Im m\ Wk_y > \pi$. It is interesting to notice that, in contrast to infinite graphene, the head-on incidence ($\Im m\ k_y \ll k_x$ occurring at $\Im m\ Wk_y \to n\pi$) is prohibited due to mixing of the longitudinal and transverse wavevectors.

There are two types of electron (hole) states in the ribbons given by the bonding and anti-bonding mixing of the sublattice wavefunctions. These strongly depend on the mirror symmetry (or lack of it) of the GNR, which follows from the tight-binding model [11]. To incorporate this feature into our model, we introduce the concept of pseudo-parity similar in nature to that in [12]:

$$\eta_{\pm K} = \begin{pmatrix} 1 \\ (\pm K 3\sqrt{3}/2\pi)^N \exp[\mathrm{i}\Im m\ (Wk_y)] \end{pmatrix}. \quad (4)$$

The pseudo-parity component of the wavefunction (1) determines whether the electron (hole) wavefunctions are either even or odd, forming bonding or anti-bonding states. Formally these can be defined by the following transformation [9]:

$$\begin{pmatrix} \Psi_b \\ \Psi_a \end{pmatrix} = \frac{1}{\sqrt{2}} \begin{pmatrix} 1 & 1 \\ -\mathrm{i} & \mathrm{i} \end{pmatrix} \begin{pmatrix} \Psi_A \\ \Psi_B \end{pmatrix}. \quad (5)$$

The pseudo-parity ensures alternation of the wavefunction sign for different bands, as shown in figure 1. In fact, the parity of $N$ determines whether or not the bonding and anti-bonding wavefunctions switch between conduction and valence bands at $K$ ($K'$) points. The electron–hole parity is comprised of the eigenvalues of the time-reversal operator:

$$s = \begin{pmatrix} 1 \\ \mathrm{sgn}\,(E - V(x)) \end{pmatrix}, \quad (6)$$

where the positive sign corresponds to electrons in the lower conduction $\pi$ band, while the negative sign stands for the holes in the highest valence $\pi^\star$ band.

The problem of tunneling through the n–p–n barrier can be described as follows. An incident particle belonging to the right moving channel ($K$ point) for $x < 0$ strikes the potential barrier at $x = 0$. The nature of the scattering determines the transmission probability density by employing continuity of the wavefunctions (1) at the junctions and conservation of the pseudo-parity $\eta_\pm$. The reflected wave contributes to the left moving channel (at $K'$). It is clear that the necessary condition for non-zero transmission is the change of the wavefunction parity under reflection. This fails for $N$ even (ZNR configuration in figure 1) and the transmission vanishes identically $t \equiv 0$. The sublattice wavefunctions (1) for $\pi$ band in the n-doped region and $\pi^\star$ band in the p-doped region have opposite signs for the pseudo-parity (opposite bonding) [14]. The situation is drastically changed for AZNR ($N$-odd) configuration. The reflected wavefunction changes its pseudo-parity while the transmitted one keeps the parity of the incident particle ($\pi$ band at $K$ and $\pi^\star$ at $K'$ have the same pseudo-parity). The transmission probability density is given by

$$t(y) = \frac{(1 - \beta)^2 \mathrm{e}^{\mathrm{i}D(k_{x,2} - k_{x,1})} A}{\beta(\mathrm{e}^{2\mathrm{i}Dk_{x,2}} - 1)(\chi^2_{A,1}\chi^2_{B,2} + \chi^2_{A,2}\chi^2_{B,1}) - (2\beta\,\mathrm{e}^{2\mathrm{i}Dk_{x,2}} + \beta^2 + 1)A}. \quad (7)$$

Here, we introduced $\beta = \exp(\mathrm{i}\pi D X_N/\sqrt{3})$ and $A = s_{B,1}s_{B,2}\chi_{A,1}\chi_{A,2}\chi_{B,1}\chi_{B,2}$; the sub-indices $A, B$ on the wavefunction components denote the corresponding sublattices. The gated (p-doped) and n-doped regions are specified by the sub-indices 2 and 1 respectively, for instance $k_{x,2}, k_{x,1}$ stand for the wavevectors along the ribbon in the p- and n-doped regions. The transmission probability (and hence, in the single channel regime, the conductance [15] in units of $2e^2/h$) is given by: $|t(k_{x,1}, k_{x,2})|^2 = \frac{1}{W}\int_0^W \mathrm{d}y\, t(y)t^\star(y)$ and shown in figure 2. It jumps up to unity at $\Re e\ k_{y,2}D = n\pi$ for any integer $n$ in the case of surface bounded holes, and at $\Im m\ k_{y,2}D = n\pi/2$ for the bulk-like holes. For the latter, there are additional resonances at $\Im m\ k_{y,2}D \to n\pi$. This situation corresponds to the quantum-dot-like states in the

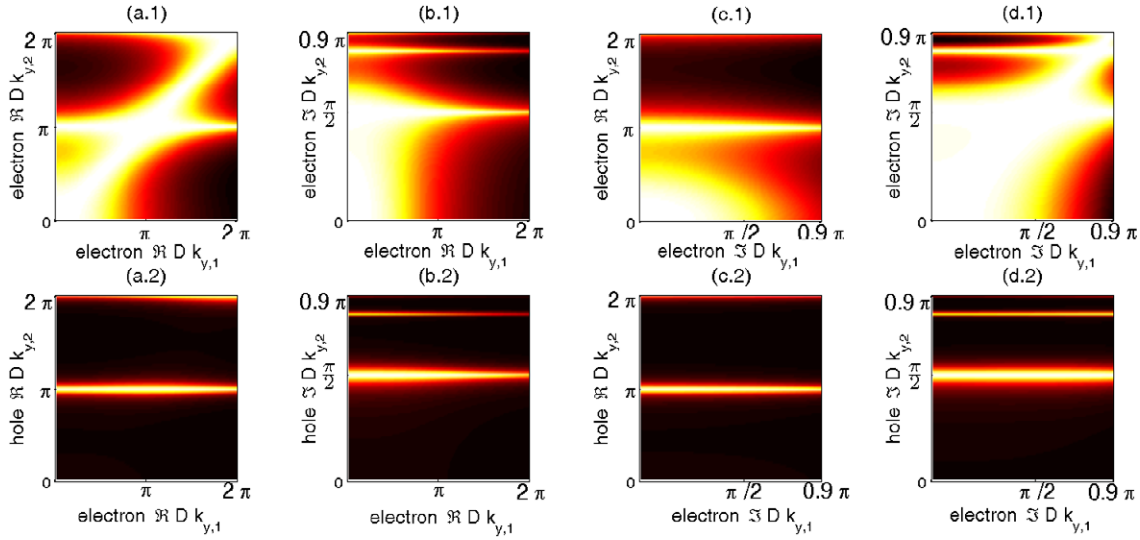


**Figure 2.** The transmission $|t(k_{y,1}, k_{y,2})|^2$ for the 9-AZNR non-chiral $\pi$ electron. Panels (a.1)–(d.1) correspond to over the barrier transmission $E > V_0$. Panels (a.2)–(d.2) represent through the barrier $E < V_0$ transmission. $\Im m\ k_{y,1(2)}$ implies that the electron (hole) is in the bulk state, while $\Re e\ k_{y,1(2)}$ signifies the surface-bound states.

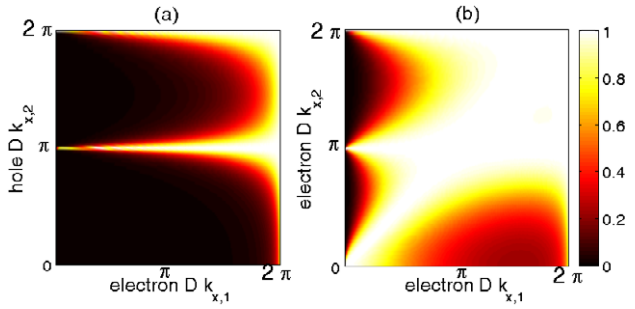


**Figure 3.** The transmission $|t(k_{x,1}, k_{x,2})|^2$ for an infinite graphene. Recall that conventionally the transmission is given in terms of the incident and refraction angles $(\phi_1, \phi_2)$ between the transverse and longitudinal wavevectors in n- and p-doped regions correspondingly. The conversion is simply given by $\lambda k_{x,1} = 2\pi \sin(\phi_1) \cot\phi_2$, $\lambda k_{x,2} = 2\pi \cos\phi_1$. As in [1], the incoming electron wavelength is taken to be equal to the width of the p-doped region. Through the barrier $E \leqslant V_0$ (a) and over the barrier $E \geqslant V_0$ (b) transmission of the chiral electron.

gated region [18]. These resonances are similar to those in infinite graphene, as shown in figure 3. The transmission is also ideal on the diagonal $k_{x,1} = k_{x,2}$ and corresponds to the absence of the gating potential.

Above we analytically demonstrated that when the Dirac fermion picture is supplemented with the concept of the pseudo-parity for ZNR (AZNR) it removes the ambiguities of the ballistic transport and correctly describes the valley-valve effect (current blocking). We now turn to the role of pseudo-parity in the Klein effect in nanoribbons. As mentioned before, the Klein paradox in infinite graphene or metallic ANR is related to the conservation of pseudo-spin projection on the particle momentum, a quantity known as chirality. That is, the through the barrier unimpeded transmission occurs at the head-on incidence, as indicated in figure 3(a) for $k_{x,1}D = 2\pi$, for all values of the gate potential $V_0$ (any $k_{x,2}D$). Transformation from the sublattice basis to the bonding/anti-bonding representation yields that the head-on incident electron is in the purely bonding state $(\Psi_a = 0)$ [1]. However, the fermions in the $\pi$ and $\pi^\star$ bands for ZNR and AZNR do not satisfy the conventional (pseudo-spin based) definition of chirality, thus often referred to as non-chiral. Furthermore, the net transmission does not demonstrate such an effect. We now turn our attention to the transmission *density* given by equation (7). It shows that at the center of the nanoribbon, the transmission density is always perfect $t(y = W/2) = 1$, regardless of the gate potential $V_0$. This effect is intimately related to the Klein paradox in infinite graphene. Since, at the nanoribbon center, the incoming wavefunctions from the sublattices $A$ and $B$ form the bonding electron state $(\Psi_a(y = W/2) = 0)$. This holds true for both edge-bound and bulk states of the $\pi$ and $\pi^\star$ bands. It follows that we can relate the unimpeded transition density to conservation of the pseudo-parity rather than conservation of the pseudo-spin in infinite graphene. In AZNR, the pseudo-parity itself defines the chirality of the fermions. The valley-valve effect of the current blockage is the other manifestation of the Klein paradox through the pseudo-parity defined chirality in ZNR.

It was also shown that, with the use of density functional theory, it is possible to obtain a more accurate band structure, which shows a gap in the ground state of zigzag nanoribbon [19]. It was also shown by Son *et al* [20] that the gap is inversely proportional to the width of the ribbon. So, for a ribbon which is wide enough the bandgap becomes negligibly small. In our model calculations, the pseudo-parity of the nanoribbon is more significant compared with the intrinsic spin. To keep the model simple, and to focus on the leading effect, we have neglected spin altogether.

In conclusion, the Klein paradox is unimpeded tunneling of the purely bonded Dirac electron state across an arbitrary wide gated region in infinite graphene. Another manifestation is perfect reflection in the graphene stacks. The paradox

is conventionally interpreted in terms of the chirality conservation. The latter is defined as a projection of pseudo-spin on the direction of motion $s \cdot p$ for the two branches originating from the sublattices. In a more general sense, the term chirality is often used to refer to an additional built-in symmetry between the electron and hole parts of the spectrum. However, in chemistry, the term chiral is used to describe an object that is non-superposable on its mirror image. These two definitions cannot be related to infinite graphene since this system has no mirror reflection symmetry. The situation is not the same for the GNR. In accordance with the chemistry definition, ZNR's are non-chiral (the mirror plane is perpendicular to the GNR plane). On the other hand, AZNR is a chiral object in the chemistry sense. It is also chiral in the sense of pseudo-parity (two opposite projections of the pseudo-parity $\eta$ on the pseudo-spin $s$). As we have demonstrated, its conservation across the n–p–n junction defines unimpeded electron tunneling at the AZNR center. Its conservation under reflection is a source of the valley-valve effect (perfect reflection) in ZNR. Both are facets of the Klein paradox in nanoribbons.

## Acknowledgments

This work was supported by contract # FA 9453-07-C-0207 of the AFRL and the Air Force Office of Scientific Research (AFOSR).

## Appendix

In this appendix, we consider the same problem for armchair nanoribbons. The wavefunction has the following form:

$$\Psi = \begin{pmatrix} \Psi_A \\ \Psi_B \end{pmatrix} = \begin{pmatrix} \exp(\mathrm{i}\mathbf{K}\cdot\mathbf{r})\exp(\mathrm{i}k_x x)\phi_A(\mathbf{r}) + \exp(\mathrm{i}\mathbf{K}'\cdot\mathbf{r})\exp(\mathrm{i}k_x x)\phi'_A(\mathbf{r}) \\ \exp(\mathrm{i}\mathbf{K}\cdot\mathbf{r})\exp(\mathrm{i}k_x x)\phi_B(\mathbf{r}) + \exp(\mathrm{i}\mathbf{K}'\cdot\mathbf{r})\exp(\mathrm{i}k_x x)\phi'_B(\mathbf{r}) \end{pmatrix}. \tag{8}$$

Here

$$\begin{pmatrix} \phi_A \\ \phi_B \end{pmatrix} = \circ \begin{pmatrix} \exp(-\mathrm{i}\phi)\exp(\mathrm{i}k_n y) \\ \exp(\mathrm{i}k_n y) \end{pmatrix} \begin{pmatrix} \phi'_A \\ \phi'_B \end{pmatrix} = s \circ \begin{pmatrix} -\exp(-\mathrm{i}\phi)\exp(-\mathrm{i}k_n y) \\ \exp(-\mathrm{i}k_n y) \end{pmatrix}. \tag{9}$$

The wavefunction $\Psi$ must be continuous at $x = 0$ and $D$ corresponding to the boundaries of the region with potential $V(x)$.

$$\begin{aligned} &\Psi(0, y; k_x, k_y; s_1; \phi) + r\Psi(0, y; -k_x, k_y; s_1; \pi - \phi) \\ &\quad = a\Psi(0, y; q_x, k_y; s_2; \theta) + b\Psi(0, y; -q_x, k_y; s_1; \pi - \theta) \\ &a\Psi(D, y; q_x, k_y; s_2; \theta) + b\Psi(D, y; -q_x, k_y; s_1; \pi - \theta) \\ &\quad = t\Psi(D, y; k_x, k_y; s_1; \phi). \end{aligned} \tag{10}$$

In the armchair case we have the same expressions connecting $k_x, k_n, \theta$ and $\phi$:

$$k_x = k_f \cos(\phi); \qquad k_n = k_f \sin(\phi) \qquad q_x = \sqrt{(E - V_0)^2 - k_n^2}; \qquad \frac{k_n}{q_x} = \tan(\theta). \tag{11}$$

Also the phase for reflected waves is $\pi$–$\phi$ compared to the phase $\phi$ for incoming wave, because only this change of phase will ensure opposite $k_x$ with the same $k_n$ according to equations (11).

In the simplest approximation when there is no $K$ and $K'$ valley mixing, the above wavefunction reduces to the four component vector

$$\Psi(\mathbf{r}) = \begin{pmatrix} \exp(-\mathrm{i}\phi)\exp(\mathrm{i}k_n y) \\ s\exp(-\mathrm{i}k_n y) \\ -\exp(-\mathrm{i}\phi)\exp(-\mathrm{i}k_n y) \\ s\exp(-\mathrm{i}k_n y) \end{pmatrix}. \tag{12}$$

This gives rise to eight equations, instead of the usual four which we need to obtain the unknowns $r, a, b, t$. Our equations may be divided into four pairs, for which both equations in each pair are equivalent. Consequently, we have the same set of simultaneous equations to solve as for the infinite graphene case, except $k_n$ across the nanoribbon is quantized and given by

$$k_n = \frac{\pi\ n}{W} - \frac{2\pi}{3a_0}. \tag{13}$$

A straightforward calculation leads to the coefficient for transmission $t = t(\phi, \theta)$ and hence the transmission probability is given by [1]

$$T = t^\star t = \frac{\cos^2(\phi)\cos^2(\theta)}{[\cos(Dq_x)\cos(\phi)\cos(\theta)]^2 + \sin^2(Dq_x)[1 - s_1 s_2 \sin(\phi)\sin(\theta)]^2}. \tag{14}$$

In the limit of a high potential barrier, i.e., $|V_0| \gg E$, the transmission (14) will become

$$T = \frac{\cos^2\phi}{1 - \cos^2(Dq_x)\sin^2(\phi)}. \tag{15}$$

The case of special interest is $W = (3N + 1)a_0$, which corresponds to the metallic subbands structure—there is no gap between the highest valence and the lowest conduction subbands. In this case $k_n = 0$ and as a result $\phi = 0$ and the expression (15) will give $T \equiv 1$—perfect transmission. For the non-metallic case we have $\sin(\phi) = \pi/k_f W$.

## References

[1] Neto A H C, Guinea F, Peres N M R, Novoselov K S and Geim A K 2009 The electronic properties of graphene *Rev. Mod. Phys.* **81** 109

[2] Geim A K 2009 Graphene: status and prospects *Science* **324** 1530–4

[3] Wang X, Ouyang Y, Li X, Wang H, Guo J and Dai H 2008 Room-temperature all-semiconducting sub-10-nm graphene nanoribbon field-effect transistors *Phys. Rev. Lett.* **100** 206803

[4] Brey L and Fertig H A 2007 Elementary electronic excitations in graphene nanoribbons *Phys. Rev.* B **75** 125434

[5] Novoselov K S, Geim A K, Morozov S V, Jiang D, Grigorieva M I K I V, Dubonos S V and Firsov A A 2005 Two-dimensional gas of massless Dirac fermions in graphene *Nature* **438** 197

[6] Novoselov K S, Jiang Z, Zhang Y, Morozov S V, Stormer H L, Zeitler U, Maan J C, Boebinger G S, Kim P and Geim A K 2007 Room-temperature quantum Hall effect in graphene *Science* **315** 1379
[7] Katsnelson M I, Novoselov K S and Geim A K 2006 Chiral tunnelling and the Klein paradox in graphene *Nat. Phys.* **2** 620
[8] Zheng H, Wang Z F, Luo T, Shi Q W and Chen J 2007 Analytical study of electronic structure in armchair graphene nanoribbons *Phys. Rev.* B **75** 165414
[9] Wakabayashi K, Takane Y, Yamamoto M and Sigrist M 2009 Edge effect on electronic transport properties of graphene nanoribbons and presence of perfectly conducting channel *Carbon* **47** 124–37
[10] Nakabayashi J, Yamamoto D and Kurihara S 2009 Band-selective filter in a zigzag graphene nanoribbon *Phys. Rev. Lett.* **102** 066803
[11] Cresti A, Grosso G and Parravicini G P 2008 Valley-valve effect and even–odd chain parity in p–n graphene junctions *Phys. Rev.* B **77** 233402
[12] Rainis D, Taddei F, Dolcini F, Polini M and Fazio R 2009 Andreev reflection in graphene nanoribbons *Phys. Rev.* B **79** 115131
[13] Kinder J M, Dorando J J, Wang H and Chan G K L 2009 Perfect reflection of chiral fermions in gated graphene nanoribbons *Nano Lett.* **9** 1980–3
[14] Li Z, Qian H, Wu J, Gu B-L and Duan W 2008 Role of symmetry in the transport properties of graphene nanoribbons under bias *Phys. Rev. Lett.* **100** 206802
[15] Akhmerov A R, Bardarson J H, Rycerz A and Beenakker C W J 2008 Theory of the valley-valve effect in graphene nanoribbons *Phys. Rev.* B **77** 205416
[16] Cheianov V V and Fal'ko V I 2006 Selective transmission of Dirac electrons and ballistic magnetoresistance of n–p junctions in graphene *Phys. Rev.* B **74** 041403
[17] Cayssol J, Huard B and Goldhaber-Gordon D 2009 Contact resistance and shot noise in graphene transistors *Phys. Rev.* B **79** 075428
[18] Trauzettel B, Bulaev D V, Loss D and Burkard G 2007 Spin qubits in graphene quantum dots *Nat. Phys.* **3** 192–6
[19] Yao Y X, Wang C Z, Zhang G P, Ji M and Ho K M 2009 A first-principles divide-and-conquer approach for electronic structure of large systems and its application to graphene nanoribbons *J. Phys.: Condens. Matter* **21** 235501
[20] Son Y W, Cohen M L and Louie S G 2006 Half-metallic graphene nanoribbons *Nature* **444** 347–9